

# On the Factorial Moment Analysis of High Energy Experimental Data with Non-integer Partition Number

Chen Gang

*Department of Physics, Jingzhou Teacher's College, Hubei 434104 China*

Liu Lianshou, Gao Yanmin

*Institute of Particle Physics, Huazhong Normal University, Wuhan 430079 China*

## ABSTRACT

It is pointed out that in doing the factorial moment analysis with non-integer partition  $M$  of phase space, the influence of the phase-space variation of two- (or more-) particle correlations has to be considered carefully. In this paper this problem is studied and a systematic method is developed to minimize this influence. The efficiency and self-consistency of this method are shown using the data of 250 GeV/ $c$   $\pi^+p$  and  $K^+p$  collisions from the NA22 experiment as example.

# 1 Introduction

Since the pioneer work of Bialas and Peschanski<sup>[1]</sup>, the anomalous scaling of factorial moments (FM) defined as

$$F_q(\delta) = \frac{1}{M} \sum_{m=1}^M \frac{\langle n_m(n_m - 1) \cdots (n_m - q + 1) \rangle}{\langle n_m \rangle^q}, \quad (1)$$

has been searched extensively in high energy experiments<sup>[2]</sup>. In the above equation,  $M$  is the partition number of a phase space region  $\Delta$  in consideration,  $\delta = \Delta/M$  is the size of a sub-cell,  $n_m$  is the number of (charged) particles falling into the  $m$ th sub-cell.

After a long period of debate, it has been recognized that in studying the anomalous scaling of FM the anisotropy of phase space should be taken into account<sup>[3]</sup>, i.e. if dynamical fluctuation does exist in high energy hadron-hadron collisions then it should be anisotropic and the corresponding fractal is “self-affine”<sup>[4]</sup>. This means that the anomalous scaling of FM can be observed when and only when the phase space is divided in an appropriate anisotropical way.

Let the three phase space variables be denoted by  $p_a, p_b, p_c$ , the corresponding shrinking ratios are  $\lambda_a, \lambda_b$  and  $\lambda_c$  respectively. The anisotropy (self-affinity) of dynamical fluctuation can be characterized by the so-called roughness or Hurst exponents<sup>[4]</sup>

$$H_{ij} = \frac{\ln \lambda_i}{\ln \lambda_j}, \quad (i, j = a, b \quad \text{or} \quad a, c \quad \text{or} \quad b, c), \quad (2)$$

with

$$\lambda_i \leq \lambda_j, \quad 0 \leq H_{ij} \leq 1. \quad (3)$$

These exponents can be deduced from the experimental data by fitting three one-dimensional second-order factorial-moments to the saturation curve<sup>[5]</sup>. If self-affine fluctuations of multiplicity do exist in multiparticle production, exact scaling, i.e. a straight line in  $\ln$ -FM versus  $\ln M$ , should be observed when and only when the three-dimensional analysis is performed with the phase space divided anisotropically according to the value of these Hurst exponents.

In order to confront this assertion with experiment, an important point has to be noticed, i.e. when  $H \neq 1$  the partition numbers  $M_i$  in the three phase space directions, in general, cannot be integer numbers simultaneously.

It turns out that the case of 250 GeV/c  $\pi^+$ p and  $K^+$ p collisions from NA22 experiments is special. The Hurst exponents determined from the one-dimensional second-order factorial-moments in these collisions are<sup>[6]</sup>  $H_{yp_t} = 0.48 \pm 0.06$  ;  $H_{y\varphi} = 0.47 \pm 0.06$  ;  $H_{p_t\varphi} = 0.99 \pm 0.01$  . These Hurst exponents can be simply approximated by  $H_{yj} = 1/2$ , ( $j = p_t, \varphi$ ), and  $H_{p_t\varphi} = 1$ . In this approximation, the following integer values for  $M_i$  can be used simultaneously in higher-dimensional analysis:  $M_y = 1, 2, 3, \dots$  and  $M_{p_t} = M_{\varphi} = 1, 4, 9, \dots$

In Ref. [6] this approximation has been used and the corresponding 3-D analysis has been performed. The self-affine 3D  $\ln F_2$  vs.  $\ln M$  thus obtained has been fitted to a straight line and the result is basically confirmative. However, it can be seen from the above that the restriction of  $M$  to integer values results in a 3-D plot with only 7 points. Omitting the first point to get rid of the influence of transverse momentum conservation<sup>[7]</sup> only 6 points remain, which are unfortunately insufficient for a precise check of the linearity of the plot.

In order to get more points in the self-affine 3-D ln-FM versus  $\ln M$  plot, non-integer values of  $M$  have to be used. In so doing an important problem arises, i.e. the influence of the variation in phase space of two- (or more-) particle correlations has to be considered carefully. In this paper we will take this problem into account and try to develop a systematic method in minimizing the influence of the deviation of two- (or more-) particle correlations from a constant behaviour.

In section 2 the definition of factorial moments with non-integer partition number  $M$  is introduced and the problem of how to use it in real experimental data analysis is discussed. It is shown that, due to the variation of two-particle correlations, a correction factor is needed. How to extract this factor from experimental data is discussed in sections 3 and 4. Concluding remarks are given in section 5.

## 2 Non-integer FM analysis

For definiteness, let us consider the second order FM in one-dimensional phase space, e.g. rapidity  $y$ :

$$F_2(\delta y) = F_2(M) = \frac{1}{M} \sum_{m=1}^M \frac{\langle n_m(n_m - 1) \rangle}{\langle n_m \rangle^2}, \quad (4)$$

where  $M = \Delta y / \delta y$ .

In the ideal case, factorial moments  $F_q$  only depend on the bin width  $\delta y$ , but not on the position of the bin on the rapidity axis. If that is the case, the result of averaging over all the  $M$  bins as in Eq.(4) is equal to that of averaging over  $N$  bins with  $N \leq M$ . That is,  $F_2(M) = F_2(N, M)$ , where

$$F_2(N, M) = \frac{1}{N} \sum_{m=1}^N \frac{\langle n_m(n_m - 1) \rangle}{\langle n_m \rangle^2}, \quad (N = M - a, \quad 0 \leq a < 1). \quad (5)$$

This equation can be used as the definition of an FM for any real value of  $M$ <sup>[8]</sup>.

As is well known, even in the central region the rapidity distribution is not flat. The shape of this distribution influences the scaling behaviour of FM. At first, Fialkowski<sup>[9]</sup> has suggested to use a correction factor to minimize this influence. Later, the cumulant variable

$$x(y) = \frac{\int_{y_a}^y \rho(y) dy}{\int_{y_a}^{y_b} \rho(y) dy} \quad (6)$$

was introduced<sup>[10]</sup>, which has a flat distribution and the Fialkowski method of correction factor has been substituted. It turns out, however, when the FM analysis with non-integer partition is concerned, a similar factor has to be introduced again.

To see this, let  $\Delta$  denote the phase space region in consideration,  $\delta_m$  the  $m$ th bin,  $\rho_1(y_1)$  and  $\rho_2(y_1, y_2)$  the one- and two-particle distribution functions, respectively. Then we have

$$\rho_1(y_1) = \frac{\langle n \rangle}{\langle n(n-1) \rangle} \int_{\Delta} \rho_2(y_1, y_2) dy_2; \quad (7a)$$

$$\langle n_m \rangle = \int_{\delta_m} \rho_1(y) dy = \frac{\langle n \rangle}{\langle n(n-1) \rangle} \int_{\Delta} dy_2 \int_{\delta_m} dy_1 \rho_2(y_1, y_2); \quad (7b)$$

$$\langle n_m(n_m - 1) \rangle = \int_{\delta_m} dy_2 \int_{\delta_m} dy_1 \rho_2(y_1, y_2). \quad (7c)$$

After transforming to the cumulant variable,  $\langle n_m \rangle$  becomes a constant, independent of  $m$ . Comparing the second and third of the above equations, it can be seen clearly that due to the difference in the integration region over  $y_2$ , even though  $\langle n_m \rangle$  is constant,  $\langle n_m(n_m - 1) \rangle$  is in general not constant.

As an example, in Fig.1 are shown  $f_2(m) = \langle n_m(n_m - 1) \rangle / \langle n_m \rangle^2$  distributions in rapidity  $y$  transformed into the cumulant variable. Data are from  $\pi^+p$  and  $K^+p$  collisions at 250 GeV/c (NA22). The four figures correspond to  $M = 8, 16, 32, 64$ , respectively. It can be seen that, although the cumulant variable has been used so that the average distribution  $\langle n_m \rangle$  is flat, the distribution of the second-order factorial moment  $f_2(m) = \langle n_m(n_m - 1) \rangle / \langle n_m \rangle^2$  is not flat.

Note that in the definition of  $F_q$ , equations (4) and (5), a horizontal average has been taken. When the partition number  $M$  is an integer, the horizontal average is over the whole region  $\Delta$ , cf. Eq.(4). The variation of  $\langle n_m(n_m - 1) \rangle / \langle n_m \rangle^2$  is thus smeared out, and no correction is needed. On the contrary, when  $M$  is non-integer, the horizontal average is performed only over part of the region, cf. Eq.(5), and the influence of the variation of  $\langle n_m(n_m - 1) \rangle / \langle n_m \rangle^2$  becomes essential. This influence is exhibited clearly in Fig.2<sup>1</sup>. In these figures,  $\ln F_2$  versus  $\ln M$  for  $y$ ,  $p_t$  and  $\varphi$  are shown with both integer (full circles) and non-integer (open circles) values of  $M$ . All these plots show a “sawtooth” shape. The “sawteeth” come from non-integer  $M$ . They lie above the smooth curve of integer  $M$  in the cases of  $y$  and  $p_t$ , but reach from above the smooth curve of integer  $M$  to below it in the case of  $\varphi$ .

In the following we will introduce a correction factor to minimize the influence of the variation of  $\langle n_m(n_m - 1) \rangle / \langle n_m \rangle^2$  and remove the “sawteeth” from the  $\ln F_2$  versus  $\ln M$  plots for real  $M$ .

---

<sup>1</sup>As in the case of integer  $M$ , the errors of the data points are correlated. This problem has been discussed in Ref.[6].

### 3 Correction factor for the $\langle n_m(n_m - 1) \rangle / \langle n_m \rangle^2$ distribution

From the definition of  $F_2(N, M)$ , Eq.(5), it can be seen that when  $M$  is non-integer ( $M = N + a, 0 \leq a < 1$ ), only  $N$  bins are included in the horizontal average, i.e. only  $r = N/M$  of the whole region  $\Delta$  has been taken into account. The result is therefore influenced by the variation of  $\langle n_m(n_m - 1) \rangle / \langle n_m \rangle^2$ . We try to minimize this influence by introducing a correction factor  $R(r)$  and define

$$F_2(M) = \frac{1}{R(r)} \left( \frac{1}{N} \sum_{m=1}^N \frac{\langle n_m(n_m - 1) \rangle}{\langle n_m \rangle^2} \right). \quad (8)$$

In order to extract the correction factor  $R(r) = R(N/M)$  from the experimental data, let us choose two integers  $N'$  and  $M'$ , satisfying

$$\frac{N'}{M'} \approx \frac{N}{M} = r. \quad (9)$$

One is then ready to calculate  $F_2(N', M')$  according to Eq.(5).

Let us call the ratio

$$C(N', M') = \frac{\frac{1}{N'} \sum_{m=1}^{N'} \langle n_m(n_m - 1) \rangle / \langle n_m \rangle^2}{\frac{1}{M'} \sum_{m=1}^{M'} \langle n_m(n_m - 1) \rangle / \langle n_m \rangle^2} \quad (10)$$

of  $F_2(N', M')$  to  $F_2(M')$  correction matrix. It is the ratio of the FM averaging only over  $N'/M'$  of the whole region to the FM averaging over the whole region. Having Eq.(9) in mind, it is reasonable, therefore, to take  $C(N', M')$  as the approximate value of the correction factor  $R(r) = R(N/M)$ .

In the left column of Fig.3 are shown the correction matrix  $C(N, M)$  with  $N$  and  $M$  both taking integer values as function of  $N/M$  for  $M = 3, 4, \dots, 40$ . It can be seen from the figures that all the points for different  $M$ 's lie in a narrow band, i.e.  $C(N, M)$  is mainly a function of  $r = N/M$  and is only weakly dependent on  $M$ . This indicates that the correction factors  $R_y(r)$ ,  $R_{p_t}(r)$  and  $R_\varphi(r)$  for non-integer  $M$  can be obtained from the interpolation of the corresponding  $C(N, M)$ 's.

It turns out that in order to eliminate the “sawteeth” in the  $\ln F_2$  versus  $\ln M$  plot appropriately, the interpolation curve should be chosen in the following way<sup>[11]</sup>: When the “sawteeth” in the  $\ln F_2$  versus  $\ln M$  plot lie above the smooth curve of integer  $M$ , as in the case of  $y$  and  $p_t$ , the upper boundary of the  $C(N, M)$  band has to be used for the interpolation; while when the “sawteeth” in the  $\ln F_2$  versus  $\ln M$  plot reach from above the smooth curve of integer  $M$  to below it, as in the case of  $\varphi$ , the middle of the  $C(N, M)$  band has to be used, cf. the dotted lines in the right column of Fig.3.

Using these interpolation curves to get the correction factors, the 1-D FM’s can be corrected according to Eq.(8). The results are shown in Fig.4. The sawteeth seen in Fig.2 are largely eliminated.

## 4 Higher-dimensional Correction

Having obtained the correction factors for one-dimensional FM’s with non-integer  $M$ , let us turn to the correction of higher-dimensional FM’s.

First, consider the 2-D case. Let  $M_1, M_2$  be the non-integer partitions in directions 1 and 2, respectively,  $N_1, N_2$  their integer parts. ( $M_1 = N_1 + a_1, M_2 = N_2 + a_2, 0 \leq a_1 < 1, 0 \leq a_2 < 1$ ). The definition of a non-integer FM, Eq.(8), is extended to

$$F_2(N_1, M_1; N_2, M_2) = \frac{1}{N_1 N_2} \sum_{m_1=1}^{N_1} \sum_{m_2=1}^{N_2} \frac{\langle n_{m_1, m_2} (n_{m_1, m_2} - 1) \rangle}{\langle n_{m_1, m_2} \rangle^2}. \quad (11)$$

The average is taken over the area  $N_1 \cdot N_2$ , shown as blank area in Fig.5a. Since the distribution of  $\langle n_{m_1, m_2} (n_{m_1, m_2} - 1) \rangle$  is in general not flat, a correction should be applied to take the shaded area in Fig.5a into account.

The one-dimensional correction factors  $R_1, R_2$  of directions 1 and 2 can take care of the areas  $\Delta S_1 = N_2(M_1 - N_1)$  and  $\Delta S_2 = N_1(M_2 - N_2)$ , respectively. However, the crossing area  $\Delta S_{12} = (M_1 - N_1)(M_2 - N_2)$  has still to be considered. We evaluate it using an area counting method. Let the area ratios be

$$b_1 = \frac{\Delta S_{12}}{\Delta S_2} = \frac{M_1 - N_1}{N_1} \quad ; \quad b_2 = \frac{\Delta S_{12}}{\Delta S_1} = \frac{M_2 - N_2}{N_2}. \quad (12)$$

The correction factor due to  $\Delta S_{12}$  can be written as

$$R_{12} = R_1^{b_2/2} \cdot R_2^{b_1/2}.$$

Noting that  $R_1 \approx 1$ ,  $R_2 \approx 1$ , we have approximately

$$R_{12} = 1 + \frac{1}{2}[b_1(R_2 - 1) + b_2(R_1 - 1)]. \quad (13)$$

The correction factor  $R^{(2)}$  for 2-dimensional FM is then

$$R^{(2)} = R_1 \cdot R_2 \cdot R_{12}, \quad (14)$$

$$F_2(M_1, M_2) = \frac{1}{R^{(2)}} F_2(N_1, M_1; N_2, M_2). \quad (15)$$

In the left column of Fig.6 are shown the 2-D FM's with real partition number  $M$  without correction. A strong "sawtooth" effect can be seen. Using correction factors obtained as above, Eq.(13-15), the large sawteeth disappear, cf. the right column of Fig.6.

Similar considerations lead to the correction factor for the 3-dimensional case, cf. Fig.5b:

$$F_2(M_1, M_2, M_3) = \frac{1}{R^{(3)}} F_2(N_1, M_1; N_2, M_2; N_3, M_3). \quad (16)$$

$$R^{(3)} = R_1 \cdot R_2 \cdot R_3 \cdot R_{12} \cdot R_{23} \cdot R_{31} \cdot R_{123}, \quad (17)$$

$$R_{12} = 1 + \frac{1}{2}[b_1(R_2 - 1) + b_2(R_1 - 1)];$$

$$R_{23} = 1 + \frac{1}{2}[b_2(R_3 - 1) + b_3(R_2 - 1)];$$

$$R_{31} = 1 + \frac{1}{2}[b_3(R_1 - 1) + b_1(R_3 - 1)];$$

$$R_{123} = 1 + \frac{1}{3}[b_1 b_2 (R_3 - 1) + b_2 b_3 (R_1 - 1) + b_3 b_1 (R_2 - 1)].$$

$$b_1 = \frac{\Delta V_{12}}{\Delta V_2} = \frac{\Delta V_{31}}{\Delta V_3} = \frac{M_1 - N_1}{N_1};$$

$$b_2 = \frac{\Delta V_{12}}{\Delta V_1} = \frac{\Delta V_{23}}{\Delta V_3} = \frac{M_2 - N_2}{N_2};$$

$$b_3 = \frac{\Delta V_{31}}{\Delta V_1} = \frac{\Delta V_{23}}{\Delta V_2} = \frac{M_3 - N_3}{N_3}.$$

The resulting 3D plots before and after correction are shown in Fig.7.

## 5 Discussion

In this paper we have developed a systematic method for an FM analysis with real (integer and non-integer) partition  $M$ . Correction factors are introduced in order to minimize the influence of the variation of  $f_2(m) = \langle n_m(n_m - 1) \rangle / \langle n_m \rangle^2$ . The corrected results for non-integer  $M$  lie on smooth curves together with the integer  $M$  points.

Note that only one-dimensional correction factors need to be extracted from the experimental data. In higher-dimensional correction the correction factors determined in one dimension have been used together with a simple geometrical consideration. This confirms the self-consistency of the method.

## Acknowledgement

The authors are grateful to Prof. W. Kittel and the NA22 Collaboration for allowing them to use NA22 data as example of the proposed method. Valuable comments on the draft from W. Kittel are highly appreciated. This work is supported in part by NSFC and the Science Fund of Hubei Province. We further thank the National Commission of Science and Technology of China (NCSTC) and the Royal Academy of Science of the Netherlands (KNAW) for support within the program Joint Research of China and the Netherlands under project number 97CDP004.

## References

- [1] A. Białas and R. Peschanski, *Nucl. Phys.* **B273**, 703 (1986), **B308**, 857 (1988).
- [2] For a recent review see E.A. De Wolf, I.M. Dremin and W. Kittel, *Phys. Rep.* **270**, 1 (1996).
- [3] Wu Yuanfang and Liu Lianshou, *Phys. Rev. Lett.* **70**, 3197 (1993).
- [4] B. Mandelbrot, *The Fractal Geometry of Nature* (Freeman, NY, 1982); T.Vicsek, *Fractal Growth Phenomena* (World Scientific, Singapore, 1989).
- [5] Wu Yuanfang and Liu Lianshou, *Science in China* **A38**, 435 (1995).
- [6] N. M. Agababyan et al. (EHS/NA22 Collaboration), *Phys. Lett.* **B382**, 305 (1996).
- [7] Liu Lianshou, Zhang Yang and Wu Yuanfang, *Z. Phys.* **C69**, 323 (1996),
- [8] Liu Lianshou, Zhang Yang and Deng Yue, *Z. Phys.* **C73**, 535 (1997),
- [9] K. Fiałkowski, B. Wosiek and J. Wosiek, *Acta Phys. Pol.* **B20**, 639 (1989).
- [10] W. Ochs, *Z. Phys.* **C50**, 339 (1991); A. Białas and M. Gazdzichi, *Phys.Lett.* **B252**, 483 (1990).
- [11] Chen Gang, Liu Lianshou and Gao Yanmin, The method of fitting correction curve for factorial moments of multiparticle production in high energy collisions (in Chinese), *HE&N Phys.* (in press).

## Figure captions

Fig.1  $f_2(m) = \langle n_m(n_m - 1) \rangle / \langle n_m \rangle^2$ , the distribution in rapidity  $y$  transformed into the cumulant variable.

Fig.2 The one-dimensional plots of  $\ln F_2$  versus  $\ln M$  for real  $M$  (from  $M = 1$  to  $M = 3.6$ ) as defined in Eq.(5). The full circles correspond to integer  $M$ , while the open circles correspond to non-integer  $M$ .

Fig.3 The correction matrix  $C(N, M)$  as a function of  $N/M$  for  $M = 3 - 40$ .

Fig.4 The one-dimensional plots of  $\ln F_2$  versus  $\ln M$  for real  $M$  (from  $M = 1$  to  $M = 3.6$ ) as defined in Eq.(5) corrected according to Eq.(8). The full circles correspond to integer  $M$ , while the open circles correspond to non-integer  $M$ .

Fig.5 Schematic plot of the phase-space area (volumn) used in the average of a two- (three-) dimensional FM for non-integer partition  $M$ . The shaded areas (volumns) are those which have to be accounted for in the correction factors.

Fig.6 The two-dimensional plots of  $\ln F_2$  versus  $\ln M$ . The left column are the results of real  $M$  as defined in Eq.(5). The right column are the results after correction.

Fig.7 The three-dimensional plots of  $\ln F_2$  versus  $\ln M$ . The left column is the result of real  $M$  as defined in Eq.(5). The right column is the result after correction.

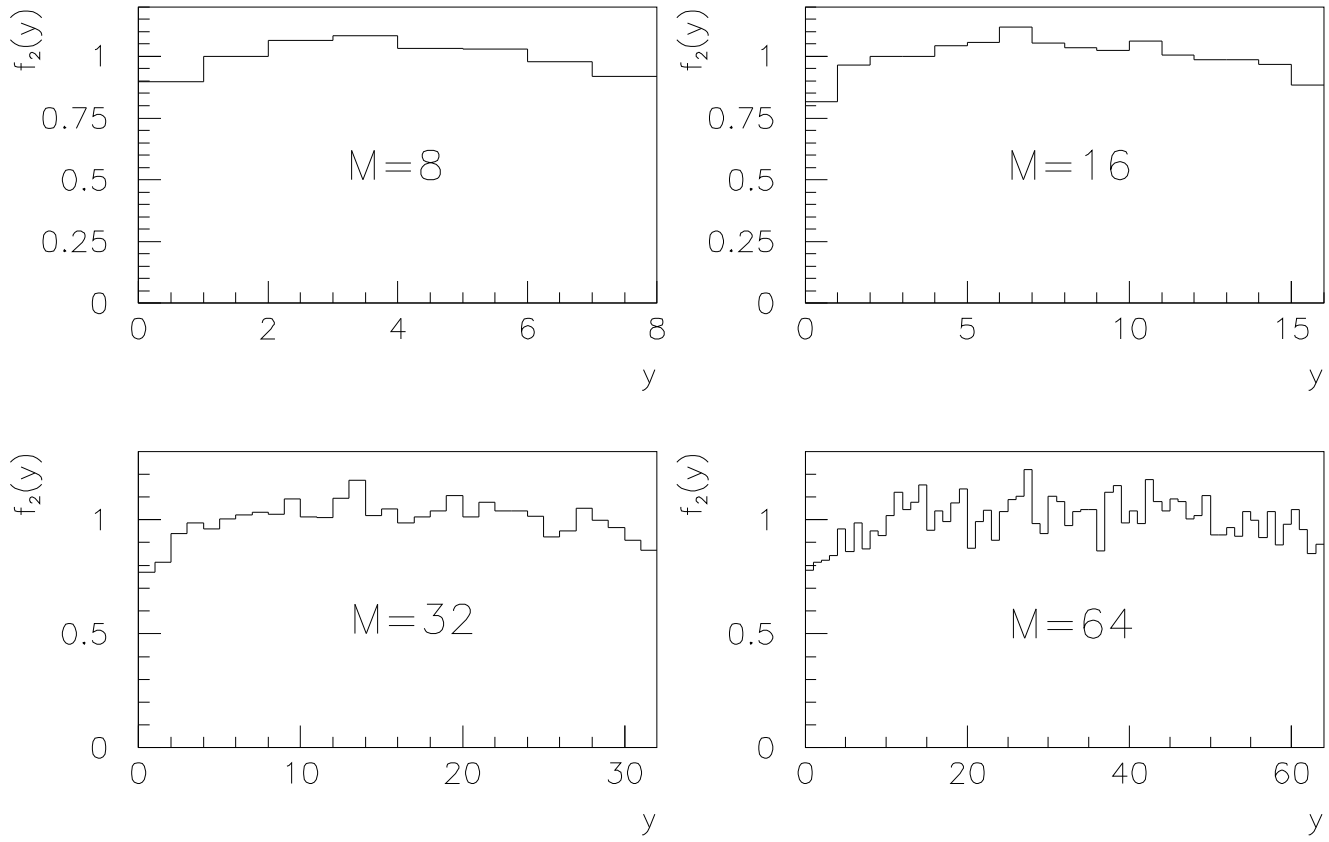


Fig.1

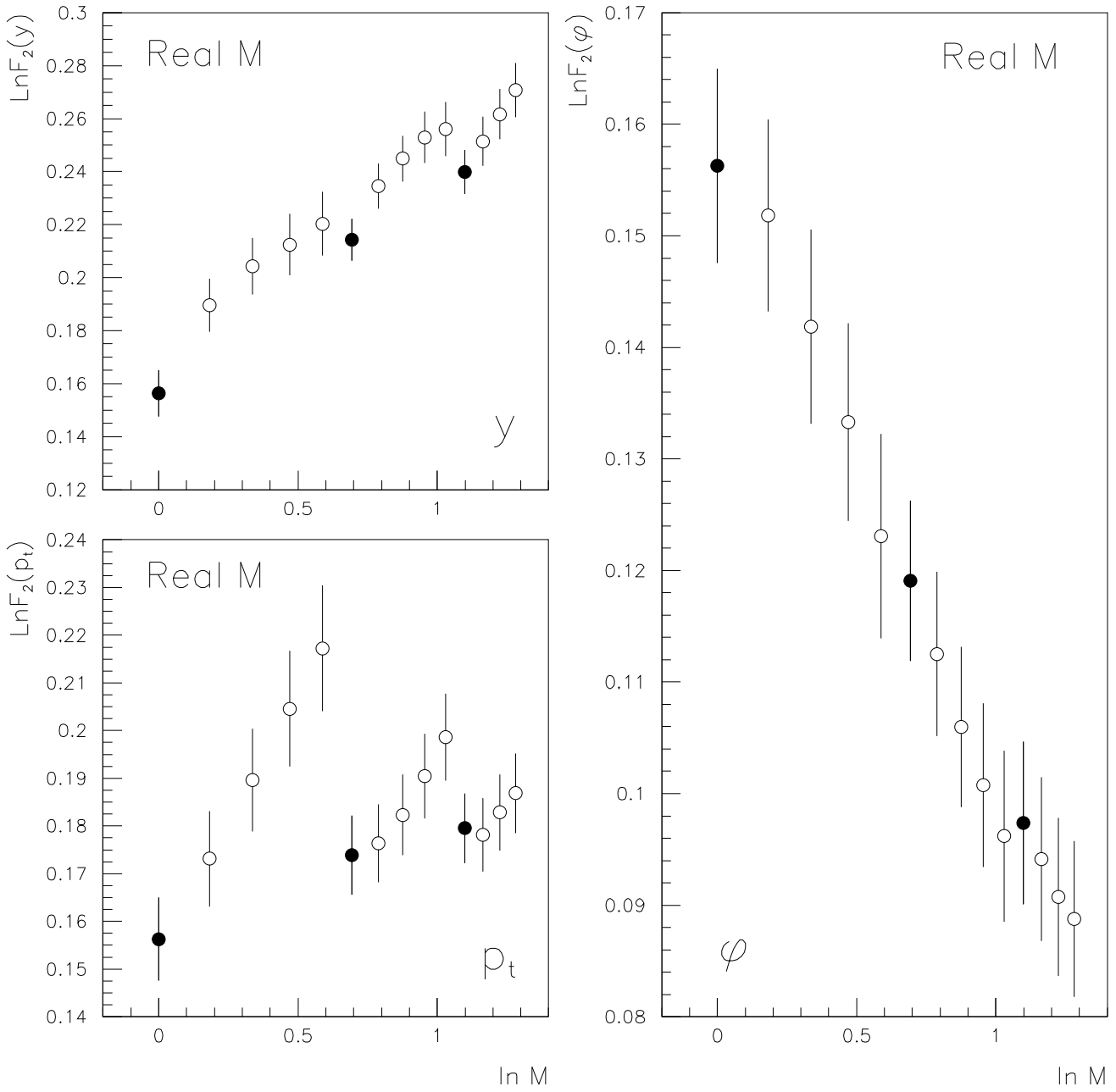


Fig.2

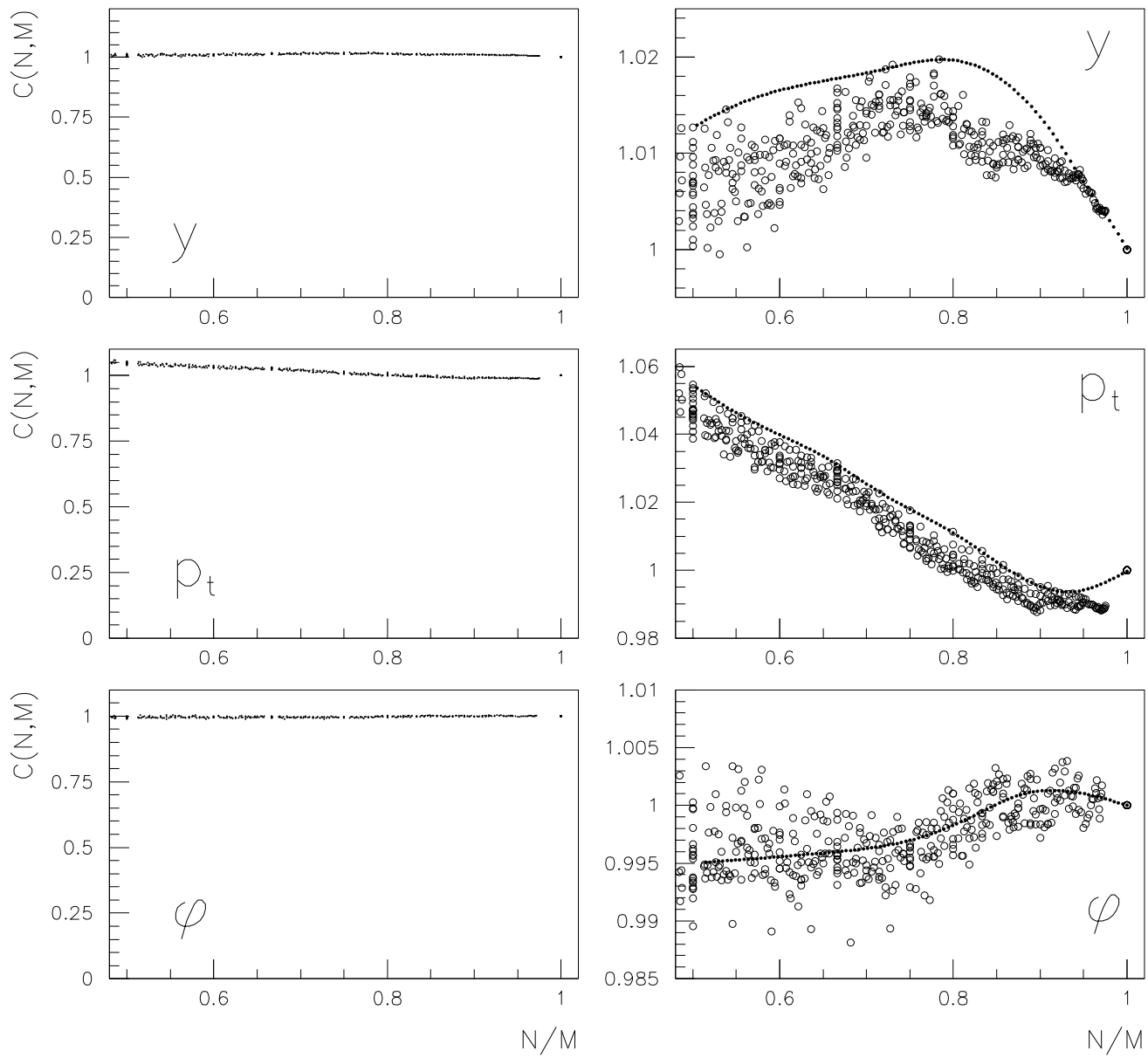


Fig.3

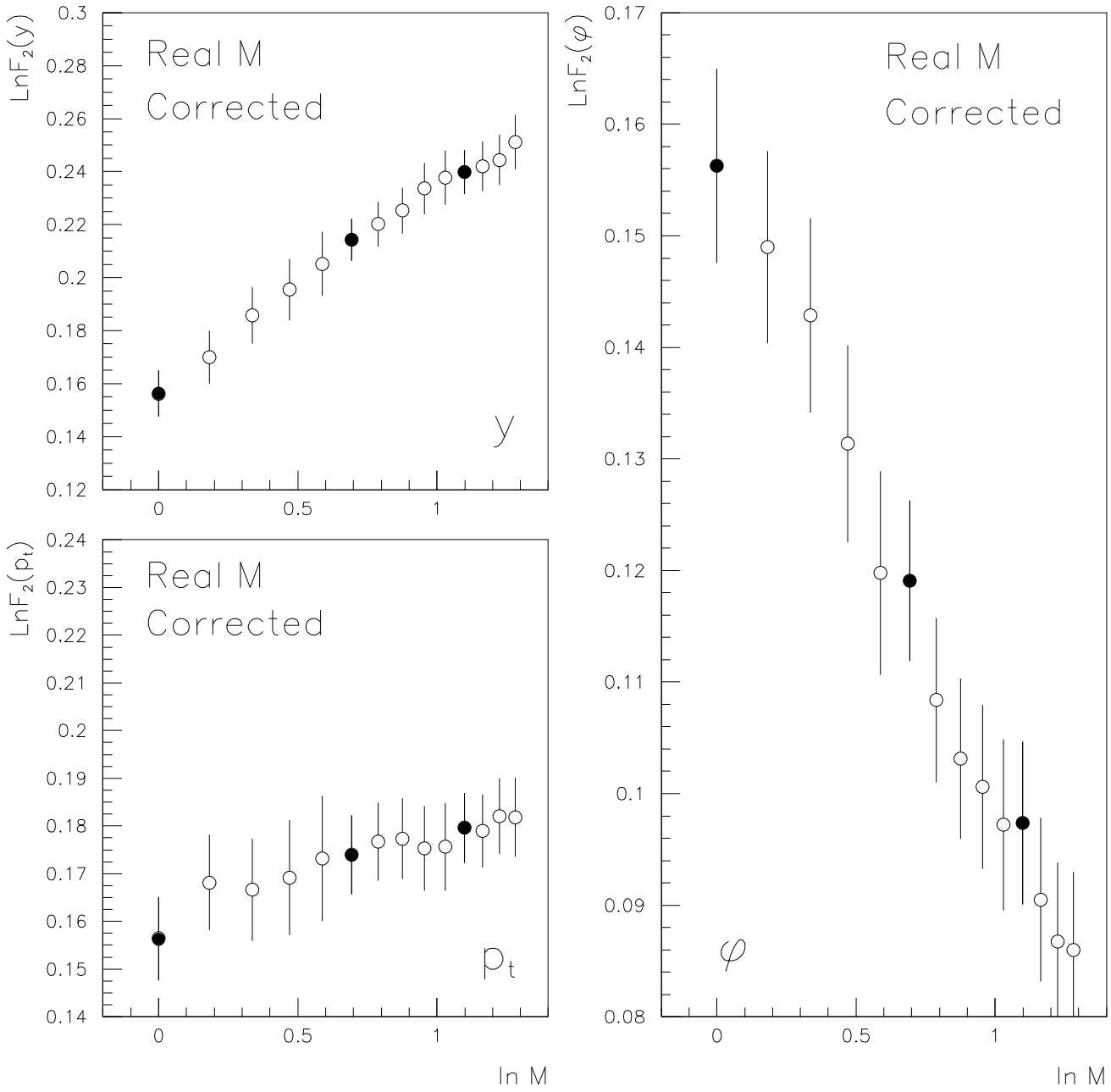
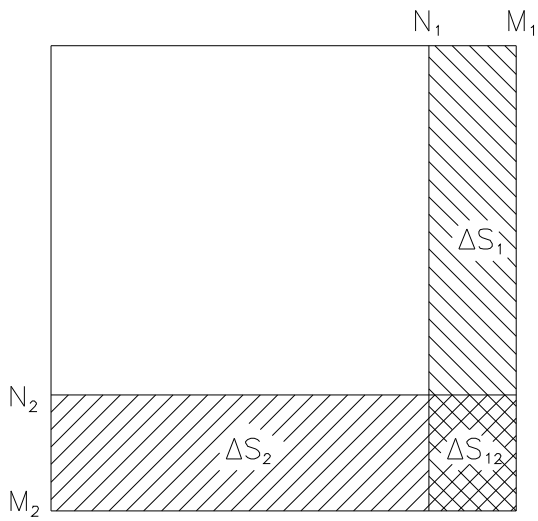
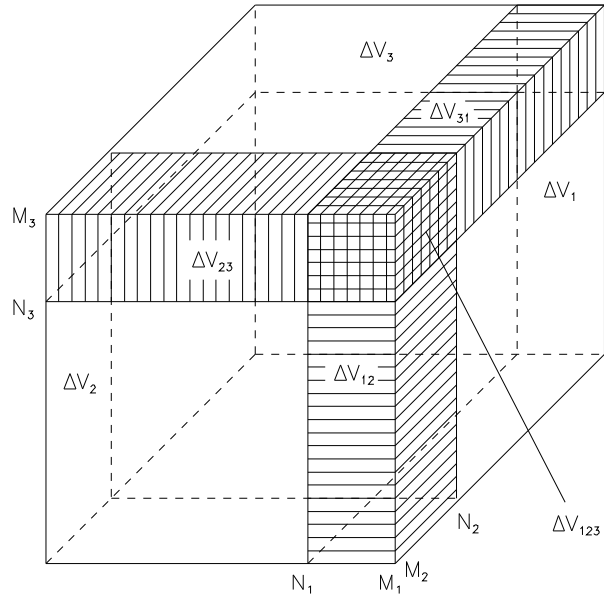


Fig.4



(a)



(b)

Fig.5

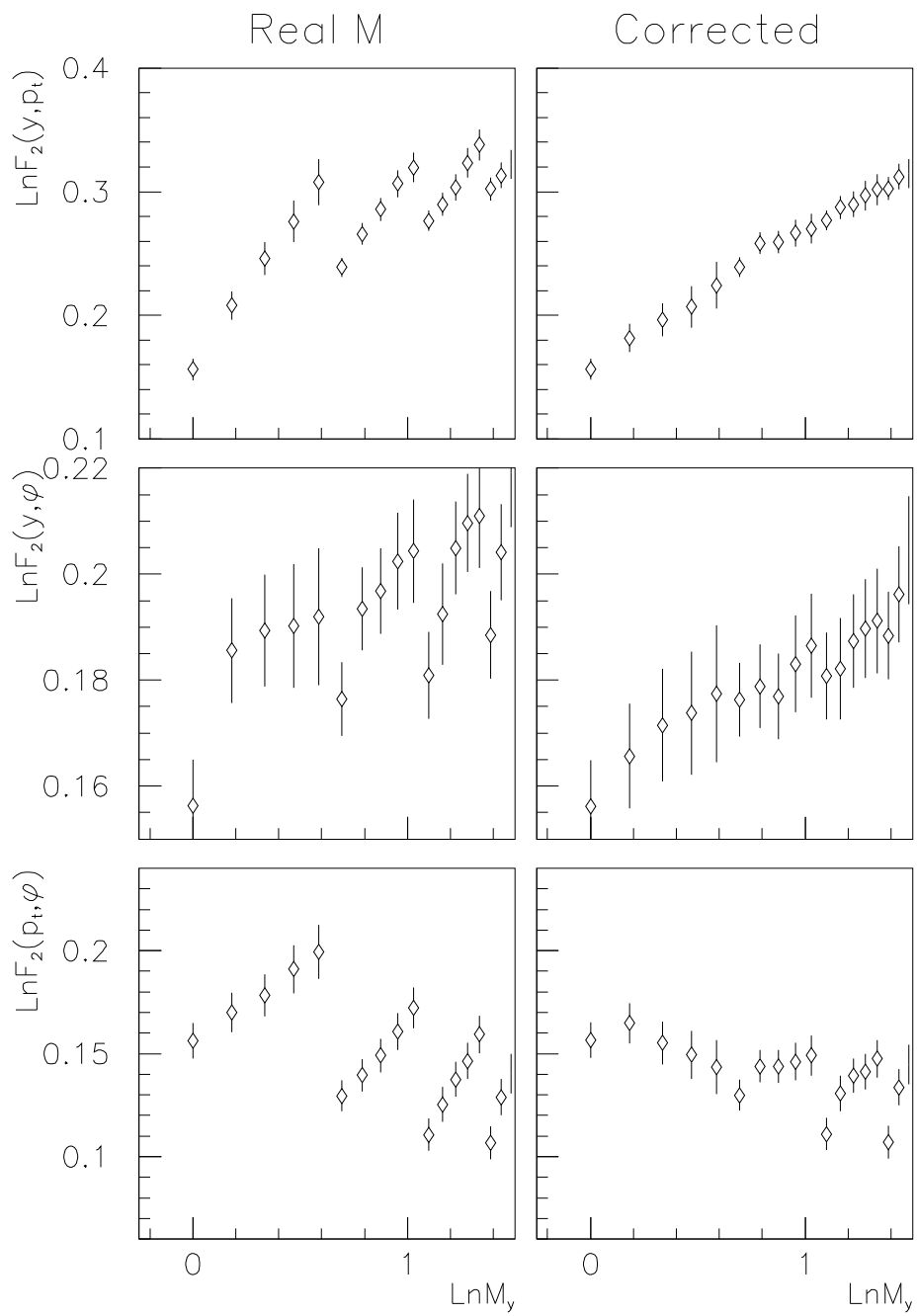


Fig.6

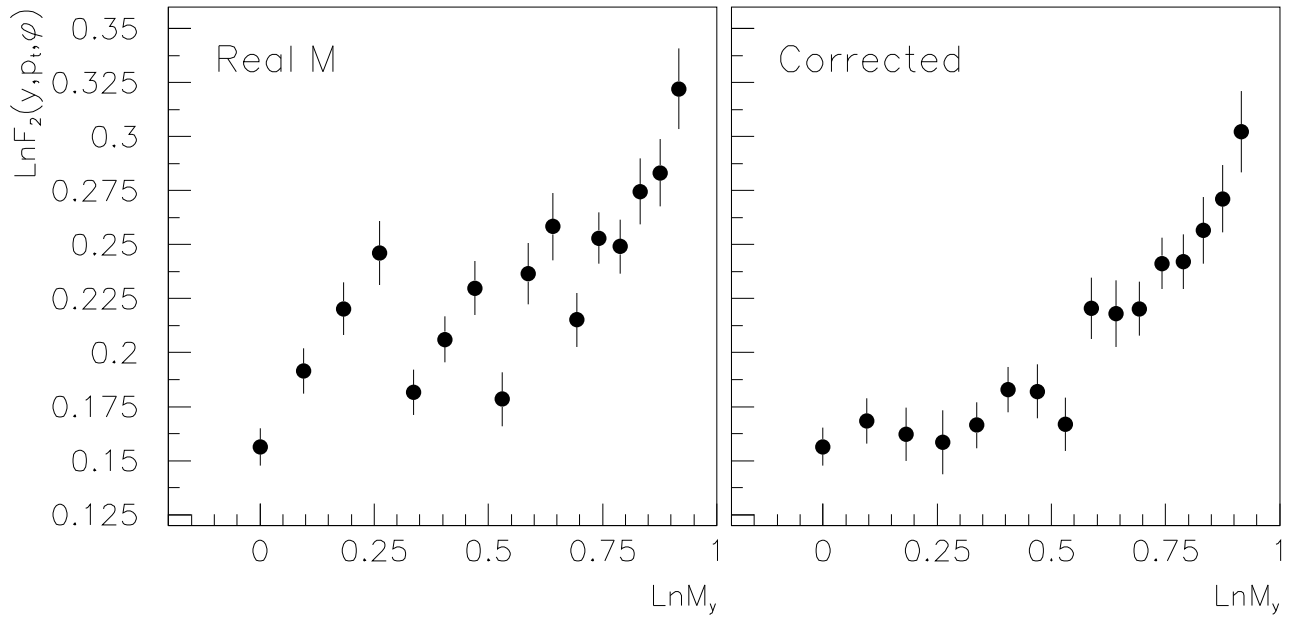


Fig.7